AGRICULTURAL RESEARCH FOUNDATION
FINAL REPORT
FUNDING CYCLE 2017 – 2019

TITLE: Development and validation of seasonal crop coefficients for Southern Oregon vineyards using the Paso Panel method

RESEARCH LEADER: Alexander D. Levin
Viticulturist and Assistant Professor
Southern Oregon Research and Extension Center
569 Hanley Rd.
Central Point, OR 97502
Phone: 541-772-5165 ext. 223
E-mail: alexander.levin@oregonstate.edu

COOPERATORS: Andy Pearl, Proprietor, Pearl Family Vineyards

EXECUTIVE SUMMARY:

Efficient irrigation scheduling is paramount to assuring a high-quality wine grape crop in Southern Oregon. As the growing season progresses, vineyard water requirements change as vine canopies develop and the environment becomes warmer and drier. While some regional growers already utilize government-provided or personal weather stations to measure environmental parameters, published values for grapevine water requirements either lack precision and/or were developed for vineyards in other regions characterized by different growing conditions and cultural practices. Therefore, in order to establish sustainable irrigation management practices in Southern Oregon, precise and reliable crop coefficients must be developed considering local management practices and climate conditions.

A field experiment was established to keep vines well-watered throughout the season. Irrigation was scheduled based on applying water at various fractions of crop evapotranspiration (ET_c) that were estimated using empirically derived crop coefficients developed for similar vineyards in California. Vine water status was monitored with regular measurements of midday stem water potential (Ψ_{stem}) over the course of the growing season to ensure that vines were not stressed for water. Canopy development over time was monitored with destructive and non-destructive methods.

The irrigation schedule successfully maintained a high water status in grapevines throughout the several seasons. Ψ_{stem} closely followed the non-stressed baseline Ψ_{stem} value that was calculated using weather data and established formulas from the literature. Canopy development occurred slowly over the first three measurement dates (4-6 weeks after budbreak), rapidly accelerated to a linear phase, then saturated approximately one month after flowering. This development pattern was common across all parameters using both destructive and non-destructive measures.

In general, canopy size saturated at a lower maximum value and at an earlier time point compared to that predicted by the crop coefficient for a vineyard of this row spacing and trellis design. Notably, the

maximum crop coefficient determined at full canopy in this vineyard was approximately two-thirds that of the predicted value from the literature. Furthermore, the maximum crop coefficient at this site was reached much earlier than predicted. At this point, it is unclear as to why this is the case, but it may be related to differences in latitude or row orientation between vineyards in California compared to Oregon. Because these crop coefficients were empirically derived in California, this is not entirely surprising. Ultimately, the implementation of crop coefficients developed in this study in Oregon vineyards can potentially result in dramatic water savings. Crop water use estimates ranged from 10 to 64% in water savings depending upon comparative estimates of wine grape water use in Southern Oregon.

OBJECTIVES:

1. Irrigate vines such that they are not stressed for water.
2. Monitor canopy development over the course of the season with destructive and non-destructive techniques.
3. Correlate and compare destructive and non-destructive measures of canopy development to calculated K_c values.
4. Develop reliable, seasonal crop coefficients for such vineyards.

PROCEDURES:

Location and plant materials. The study was conducted in a 12 ha. *Vitis vinifera* L. cv. Pinot noir vineyard located in the Applegate Valley near Wilderville, Oregon (42°23'5.53"N, 123°27'27.90"W) planted in 2009. The vines were grafted on 101-14 rootstock. The rows were oriented approximately north-south with a spacing of 2.4 m x 1.2 m (row x vine) for a vine density of approximately 3472 vines per hectare. The vines were trained to bilateral cordons and spur-pruned. Shoots were thinned to a density of ~25 shoots per meter. The foliage is grown on a vertically shoot positioned (VSP) trellis with a fruiting wire at 0.9 m above the soil surface, and three foliage catch wires at 1.2, 1.8, and 2.1 m above the soil surface. The shoots were hedged once they grow 0.3 m beyond the upper wires of the trellis.

Experimental treatments and design. A previously established irrigation experiment was utilized for the determinations made in this study. The experiment consisted of eight different irrigation treatments characterized by varying rates of irrigation based on fractions of crop evapotranspiration (ET_c) either before or after veraison (onset of ripening). Treatment descriptions are as follows:

- Wet control (WC) – 100% ET_c from anthesis until harvest.
- Dry control (DC) – 25% ET_c from anthesis until harvest.
- Early deficit 75% (ED_{75}) – 75% ET_c preveraison; 100% ET_c postveraison.
- Early deficit 50% (ED_{50}) – 50% ET_c preveraison; 100% ET_c postveraison.
- Early deficit 25% (ED_{25}) – 25% ET_c preveraison; 100% ET_c postveraison.
- Late deficit 75% (LD_{75}) – 100% ET_c preveraison; 75% ET_c postveraison.
- Late deficit 50% (LD_{50}) – 100% ET_c preveraison; 50% ET_c postveraison.
- Late deficit 25% (LD_{25}) – 100% ET_c preveraison; 25% ET_c postveraison.

The experimental design was a randomized complete block design with five replications. Each block was 24 vines in length and eight rows across, for a total of 192 vines per block. Blocks were replicated down the rows. The treatment plots were randomized within each block and were six vines in length and four rows across, for a total of 24 vines per plot. Data were collected from the center eight vines (four vines of two center rows) of each plot. Thus, each plot was encircled by a ring of border vines. Only the WC treatment was used for this study, thus a total of 40 vines was used for data collection (eight vines per experimental unit x five replications).

Applied water amounts and vine water status. Water was applied to the vines using four 2 L $hr.^{-1}$ drip emitters per vine placed on each side of the trunk approximately 0.3 m above the soil surface. Vines

were irrigated at 100% ET_c, which was estimated using the following equation: $ET_c = ET_o * K_c$, where ET_o is reference ET and K_c is the crop coefficient. Reference ET was obtained from a weather station (Vantage Pro 2, Davis Instruments) located at the research site. Variables measured and calculations used to determine daily ET_o can be found in Snyder and Pruitt (1992). The crop coefficient was calculated from accumulated growing degree-days from 1 April (base 10°C) using the following VSP-specific equation developed by (Williams, 2014) and adjusted for 2.4 m row spacing (Fig.1).

To ensure that plants were not stressed for water, weekly measurements of Ψ_{stem} were made and compared to baseline non-stressed Ψ_{stem} values. Ψ_{stem} was measured using a pressure chamber (Model 610, PMS Instruments, Corvallis, OR) as described by Williams and Araujo (2002). Briefly, Ψ_{stem} measurements were taken between 1230 and 1330 h Pacific Daylight Time. Leaves chosen at the time of measurement were fully expanded, mature leaves exposed to direct solar radiation. Leaf blades were covered with an opaque Mylar plastic bag and quickly sealed after excess air was squeezed out of the bag. After 30 minutes, bagged leaves were excised and pressurized within 10 to 15 seconds. A single leaf from each plot was measured and used for data analysis. Baseline non-stressed Ψ_{stem} values were calculated from vapor pressure deficit data at the time of measurement using the equation from Figure 3 in Williams and Baeza (2007). Irrigation commenced once midday stem water potential (Ψ_{stem}) reached -0.8 MPa.

Canopy measurements. Estimates of primary and secondary leaf area were made according to the method of Williams et al. (2003). Briefly, on each measurement date, a minimum of 40 individual shoots of varying lengths were collected from similarly irrigated surrounding vines and brought back to the laboratory. The length of each sampled shoot was measured, and leaf area determined with a leaf area meter (LI-3100C, LICOR Biosciences, Lincoln, NE). The relationship between shoot length and total leaf area was established via regression analysis. In the field, the lengths of two representative shoots will be measured on vines within each experimental unit. Total leaf area of vines in each experimental unit will then be calculated based upon the relationship between shoot length and leaf area and multiplied by the number of shoots per vine. Total number of shoots per vine was determined after shoot thinning practices were completed.

The two experimental methods were used to determine canopy shaded area: either by digital image method as in Williams and Ayars (2005), or by the *Paso Panel* method as in Battany (2006). Paso Panel measurements will be taken underneath each cordon of vines within an experimental unit, while digital image measurements will be taken underneath two cordons of all adjacent vines within an experimental unit. Shaded area measurements using each method were made at key times during canopy development.

SIGNIFICANT ACCOMPLISHMENTS:

Objective 1: Irrigate vines such that they are not stressed for water

Heat accumulation. Daily total degree days (DD day^{-1}) increased throughout each growing season from approximately 2.5 DD day^{-1} at the beginning of the season to a maximum of just over 15 DD day^{-1} in midsummer. In both seasons, the peak maximum daily heat accumulation at the study site occurred in

late-July/early-August, though the peak was two weeks earlier in 2018 compared to 2017. Following the seasonal peak, DD day-1 decreased rapidly until harvest, at which point it was approximately 7.5 DD day-1 (Fig. 2). Overall, 2017 was only slightly warmer than 2018, with 1752 and 1720 degree days from 1 April to 31 October in 2017 and 2018, respectively.

The presence of wildfire smoke in both years impacted daily heat accumulation patterns differently. In 2017, the smoke was present during the last three weeks of August and into the first week or so of September. This modulated the decrease in daily heat accumulation and is shown by a flattening of the curve during this time (Fig. 2). Moreover, the smoke more or less stabilized the daily fluctuations in temperature, probably due to the insulating effect of the smoke. However, in 2018, the smoke arrived much earlier in the growing season (~15 July) and lasted longer (~5 weeks). This explains the earlier seasonal peak in DD day^{-1} – as the smoke tends to reduce daily maximum temperatures – yet the smoke did not seem to modulate the reduction in heat accumulation over time quite as much as in 2017.

Environmental water supply and demand. As is typical of this growing region, most of the seasonal rainfall occurred during the winter months, with very little precipitation during each growing season (Fig. 3). Approximately 223 and 162 mm fell from 1 April to 31 October in 2017 and 2018, respectively. However, 91% and 97% of growing season rainfall fell prior to fruit set and after harvest in 2017 and 2018, respectively. Also, as is typical for the region, mid-summer thunderstorms (often without significant rainfall) ignited wildfires in both years – early-August in 2017, and mid-July in 2018 (Fig. 3).

Daily evaporative demand (ET_o; mm day^{-1}) generally followed the pattern of total daily solar radiation throughout the growing season. ET_o increased from 2.5 to 3.0 mm day^{-1} at the beginning of the growing season to a peak in late-June of 6.0 to 6.5 mm day^{-1} (Fig. 4). The daily values of ET_o varied widely during the late-Spring/early-Summer months of the growing season, due to varying cloud cover and wind as is associated with Spring weather. Weekly ETo values gradually decreased from the seasonal peak in late-June towards the end of the growing season at the end of the October by approximately 0.2 mm $week^{-1}$. Notably, daily ETo values in 2017 (in early-August/early-September) and in 2018 (mid-July/early-September) were significantly reduced, due to the reduction in solar radiation caused by the presence of wildfire smoke, though the impact was greater in 2018 (Fig. 4). From 1 May to the end of the growing season, ET_o totaled 771 mm for both years.

Estimated vine water use. Estimated daily vine water use (ET_c) increased exponentially from 1 April until a peak in mid-summer (Fig. 5). However, the peak was reached nearly a month earlier and was of significantly lower magnitude in 2018 (< 2.5 mm day^{-1}) compared to 2017 (> 3.0 mm day^{-1}). Again, this was attributed to the presence of wildfire smoke in the atmosphere. The smoke arrived later in 2017, and upon intercepting solar radiation, ETc significantly decreased from early-August to early-September (Fig. 5). When the smoke cleared, ETc increased slightly for a brief period, but then slowly decreased towards the end of the season. In 2018, ET_c flat-lined in mid-July upon arrival of the smoke and was kept below 3.0 mm day^{-1} until early-September. Overall, total seasonal estimated ET_c was similar between the two years (330 mm).

Vine phenology. Timepoints of phenological events were similar between the two growing seasons of this study, with few notable differences (Table 1). Budbreak was later than normal in both years, with 50% budbreak observed in vines on 17 April in 2017 and 23 April in 2018. However, bloom was nearly two weeks earlier in 2018 compared to 2017 (31 May vs. 12 April). Veraison was observed at the study site on almost the exact same day in each year (14 and 13 August in 2017 and 2018, respectively. Harvest also occurred on almost the same day in each year (26 and 24 September in 2017 and 2018, respectively). Notably, harvest occurred 106 days after bloom in 2017, but 116 days after bloom in 2018.

Applied water amounts. Irrigation began when midday stem water potential reached -0.8 MPa – averaged across experimental plots – in each year of the study. In general, applied water amounts were similar between the two years, with slightly more water applied in 2018 (Table 2). Applied water from the initiation of irrigation through harvest was 674 and 761 L vine^{-1} in 2017 and 2018, respectively. The balance between total estimated ET_c and total applied water (~265 L or 89 mm) is assumed to have come from stored soil moisture.

In 2017 and 2018, irrigation began on 10 July and 16 July, respectively. Slightly less water was applied during the preveraison period in 2018 compared to 2017, whereas slightly more was applied during the postveraison period (Table 2). Total preveraison applied water amounts were 360 and 318 L vine^{-1}, in 2017 and 2018, respectively. Total postveraison applied water amounts were 314 and 443 L vine^{-1} in 2017 and 2018, respectively.

Seasonal vine water status. Vine water status (midday Ψ_{stem}) was monitored in WC plots from late-May to harvest in each growing season to determine if vines were stressed for water during the experiment (Fig. 6). In 2017, Ψ_{stem} values ranged from -0.3 to -0.6 MPa in WC plots, with the lowest values recorded in late-July. Measured values were only significantly below the calculated non-stressed baseline on one measurement date in late-July in 2017. In 2018, Ψ_{stem} values ranged from -0.4 to -0.8 MPa, with lowest values measured in mid-July. Compared to 2017, many more measurement dates (from early-July to late-August) showed that vines were significantly below the non-stressed baseline value, indicating some water stress. However, vine water status never fell below -0.8 MPa, suggesting that the water stress experienced was not severe enough to reduce shoot elongation and thus canopy development.

Objective 2: Monitor canopy development over the course of the season with destructive and non-destructive techniques

In 2017, shoot growth, leaf area, and canopy development were monitored using destructive and non-destructive techniques. In 2018, only non-destructive techniques were used.

Shoot growth and leaf area development. Shoot length was a significant function of growing degree days after budbreak (GDD). Data were well fit with a sigmoidal function (R^2 = 0.99). Shoot length increased slowly from budbreak up to 200 GDD, before reaching at maximum growth rate at 245 ± 10 GDD from budbreak, which was in late May, just prior to bloom. Shoots continued to grow rapidly until reaching 95% of their maximum estimated length (162 ± 5 cm) at approximately 450 GDD (Fig. 7). Shoots were hedged twice before harvest – just after measurements on 10 July and 14 August – and the data taken from these dates was not included in the regression. The final measurement on 28 August occurred at 1368 GDD from budbreak and shoot length was 153 ± 11 cm.

Seasonal evolution of leaf area per vine followed similar patterns to shoot length (Figure 8) and was a strong significant linear function ($P < 0.001$) of primary shoot length (Figure 9). Primary leaf area development proceeded slowly from the first measurement date, and also equaled the total leaf area per vine for the first three measurement dates since no secondary leaf area was present. Primary and total leaf area continued to increase linearly until 10 July (621 GDD), although total leaf area increased more rapidly as a fraction of the total was made up of secondary leaf area. The first measurements of secondary leaf area were made on 2 June. Secondary leaf area increased linearly until 10 July also, then leveled off (as did total and primary leaf area). At the last measurement date (28 August), total, primary, and secondary leaf area equaled 5.5, 4.1, and 1.3 m^2/vine, respectively. Thus, secondary leaf area equaled just over one fifth of the total leaf area per vine.

The sigmoidal curves modeling total, primary, and secondary leaf area development were well fit to the data, R^2 values of 0.99, 0.98, and 0.86 for total, primary, and secondary leaf area functions, respectively. The modeled curves show that secondary leaf area reached 95% of its maximum value between 350 to 400 GDD (corresponding to the third week of June at this site in 2017), while primary leaf area reached 95% of its maximum value from 400 to 450 GDD (corresponding to the fourth week of June at this site in 2017). The final measured values of leaf area (given above) all fell within the 95% confidence interval of the parameter estimates for curve asymptotes, which represent a modeled maximum value of leaf area. Thus, these equations could be used to predict leaf area development at this site going forward and have potential utility for modeling leaf area development in similar vineyards in the region, though more work is required to validate the data.

Canopy shaded area. Canopy percent shaded area (PSA) followed similar developmental patterns to primary shoot growth and total leaf area and was a significant function ($P < 0.001$) of GDD in each year (Figure 10; Table 3). ANOVA showed that measurement method also significantly ($P < 0.001$) affected the values of PSA in each year. Finally, the significant interaction ($P < 0.001$) between degree days and method (DD * M) indicates that the significant differences between measurement methods depended on GDD.

The Levene's ANOVA was conducted on the absolute values of model residuals to determine if there were any significant differences in variance among treatment groups prior to regular ANOVA (Table 3). The test resulted there were no significant differences in variance among any of the main or interaction effects in each year ($P > 0.05$). This indicates that variance in the measured values of PSA did not change significantly over the growing season and was not significantly difference due to measurement methods among all treatment groups. Importantly, this suggests that both measurement methods were equal in terms of precision for measuring PSA.

Pairwise comparisons between measurement methods were conducted at each measurement date in each year (Table 4). At a majority of timepoints in each year, the Paso panel method (PP) returned a significantly higher estimate of PSA compared to the Shade board method (SB). Only two dates in 2019 did the PP method return significantly *lower* values of canopy PSA. The yearly average estimates (calculated across measurement dates within a given year) were similar across years with estimates of

0.39, 0.32, and 0.31 for 2017, 2018, and 2019, respectively. This indicates that on average the PP method was consistently measuring higher PSA values year-to-year.

Objective 3: Correlate and compare destructive and non-destructive measures of canopy development to calculated K_c values.

Non-destructive measures of canopy development using the two measurement methods were well correlated to destructive measures. In general, canopy PSA was a significant function of primary shoot length (Fig. 11) and total vine leaf area (Fig. 12) for both the PP and SB methods. However, the relationships of PSA to both primary shoot length and total vine leaf area were better fit with the SB method. Slopes of regression lines were similar between methods, though intercepts were slightly higher for the PP method, indicating a higher estimate of canopy PSA. This was confirmed by correlating canopy PSA measured by PP over canopy PSA measured by SB (Fig. 13). Though the slope of the regression line was not significantly different than 1:1 – indicating that both methods accurately captured canopy PSA development over time – the intercept of the regression line was 6.7 – suggesting that the PP method estimated canopy PSA at approximately 6.7% higher than SB.

Objective 4: Develop reliable, seasonal crop coefficients for such vineyards.

Canopy PSA as determined by both measurement methods was converted to K_c using the modified equation from Williams and Ayars (2005) – $K_c = PSA * 0.017$. A non-linear mixed model was used to fit a three-parameter sigmoidal function through three years of data for each method (Fig. 14). All parameters were allowed to vary with the fixed effect of measurement method and with the random effect of block.

Function parameters were estimated for each measurement method (Table 6). The function asymptotes – representing seasonal maximum K_c values; K_c^{max} – were estimated (± standard error; SE) to be 0.34 ± 0.02 and 0.46 ± 0.02 for the SB and PP methods, respectively. The function inflection points – representing the GDD from budbreak when K_c was 50% of maximum; K_c^{50} - were estimated to be 294 ± 25 and 269 ± 19 for the SB and PP methods, respectively. Finally, the function scalar parameters – a unitless parameter representing the linear portion of the curve – were estimated to be 105 ± 22 and 114 ± 18 for the SB and PP methods, respectively. The scalar parameter value is equal to $(\Delta K_c^{75\text{-}25} - 0.002)*2.196^{-1}$, where $\Delta K_c^{75\text{-}25}$ is the difference in K_c between 75% and 25% of K_c^{max}.

Pairwise comparisons were conducted between parameter estimates to determine whether or not any were significantly different between measurement methods (Table 7). K_c^{max} was significantly higher for PP compared to SB by 0.12 ± 0.02 ($P < 0.001$). There were no significant differences between methods for the other two parameters.

A new reduced model was fit to the data that eliminated K_c^{50} and the scalar parameters from both fixed and random effects, then statistically compared to the original model. The new, more parsimonious model was not-significantly different than the original more complex model ($P = 0.9741$). New estimates were obtained for all function parameters (Table 8). A common K_c^{50} and scalar parameter were fit for both methods – 280 ± 15 for K_c^{50} and 110 ±14 for the scalar – along with the same separate

K_c^{max} values as estimated from the first model. The greater degrees of freedom in the new model resulted in slightly smaller confidence intervals for all fitted parameters. New equations for K_c are shown in Fig. 15 as a function of GDD from 1 April.

Utilizing the new equations for each method, crop water use (ET_c) was modeled for wine grapes from 1 April to 31 October using 30-year averages for ET_o and GDD obtained from the AgriMet weather station at SOREC (Fig. 16). ET_c was modeled for grapes grown on 8 ft. row spacing with a VSP trellis and north-south oriented rows as was used in the study. This is also a common vineyard design used statewide and was recently used for a vineyard cost of production study published by OSU (Olen and Skinkis, 2018).

Over the course of the entire growing season, K_c equations developed in this study resulted in significantly lower estimates of crop water use for wine grapes by 10 to 33% compared to that estimated by Williams (2014). This study estimated yearly wine grape ETc to range from 216 to 292 mm/year (8.5 to 11.5 in.). In contrast, the VSP K_c equation from Williams (2014), estimated yearly wine grape ET_c for this region to be 323 mm/year (12.7 in). Furthermore, the estimated daily ET_c from this study reached its (lower) maximum value three weeks earlier in the growing season. Maximum daily ET_c estimated from this study was 1.99 to 2.69 mm/day and achieved on 21 July, whereas the Williams (2014) maximum daily ET_c estimate of 2.87 mm/day was achieved three weeks later on 14 August.

BENEFITS & IMPACT:

The ultimate benefit from this study is the development of new crop coefficients for improved wine grape irrigation scheduling in Oregon. The equations underlying these new crop coefficients were developed over the course of three growing seasons in a representative vineyard – Pinot noir grapevines grafted on to 101-14 rootstock planted on an 8 ft. row spacing and foliage trained to a VSP trellis system. These characteristics are shared among a vast majority most vineyards in throughout Oregon. Thus, the crop coefficients generated herein would have the broadest potential application statewide.

By implementing the new crop coefficients generated in this study into an updated irrigation schedule, potential water savings in vineyards was calculated to range from 10 to 33% over existing crop coefficients for similar vineyards obtained from the literature (12.7 in.). Moreover, the calculated crop water use in this study (8.5-11.5 in./year) would be 51 to 64% lower than the historical (2003-2015) crop water use figures for wine grapes provided by AgriMet in Medford (23.6 in./year). Given that a significant portion of early season crop water use comes from stored soil moisture, the ultimate reduction in actual applied water amounts in Oregon vineyards would be significantly reduced. Despite these reductions, vines were shown to be not stressed for water, and yielded well above the state average tonnage in 2017 and 2018 (> 5 tons per acre).

ADDITIONAL FUNDING RECEIVED DURING PROJECT TERM:

Additional awards of ~$100,000 was granted by the Oregon Wine Board (OWB) in 2017 and 2018 to conduct parallel research on the effects of water deficits on fruit yield and quality at this study site.

FUTURE FUNDING POSSIBILITIES:

With the promising pilot data generated from this study, additional funding will be sought from state and federal sources to validate and continue to improve crop water use estimates.

Literature Cited

Battany, M.C., 2006. A rapid method for measuring vine canopy shaded areas, Grape Notes. University of California Cooperative Extension, San Luis Obispo, CA.

Olen, B., Skinkis, P.A., 2018. Vineyard Economics: Establishing and Producing Pinot noir Wine Grapes in the Willamette Valley, Oregon. Oregon State University Extension Service.

Snyder, R.L., Pruitt, W.O., 1992. Evapotranspiration data management in California., Water Forum: Irrigation and Drainage Session. ASCE, Baltimore, MD, pp. 128-133.

Williams, L.E., 2014. Determination of Evapotranspiration and Crop Coefficients for a Chardonnay Vineyard Located in a Cool Climate. American Journal of Enology and Viticulture 65, 159-169.

Williams, L.E., Araujo, F.J., 2002. Correlations among Predawn Leaf, Midday Leaf, and Midday Stem Water Potential and their Correlations with other Measures of Soil and Plant Water Status in *Vitis vinifera*. Journal of the American Society of Horticultural Science 127, 448-454.

Williams, L.E., Ayars, J.E., 2005. Grapevine water use and the crop coefficient are linear functions of the shaded area measured beneath the canopy. Agricultural and Forest Meteorology 132, 201-211.

Williams, L.E., Phene, C.J., Grimes, D.W., Trout, T.J., 2003. Water use of mature Thompson Seedless grapevines in California. Irrigation Science 22, 11-18.

Figure 1. Evolution of crop coefficient as a function of accumulated degree days (base 10ºC) from 1 April. Equation taken from Williams (2014) and adjusted for 8 ft. row spacing.

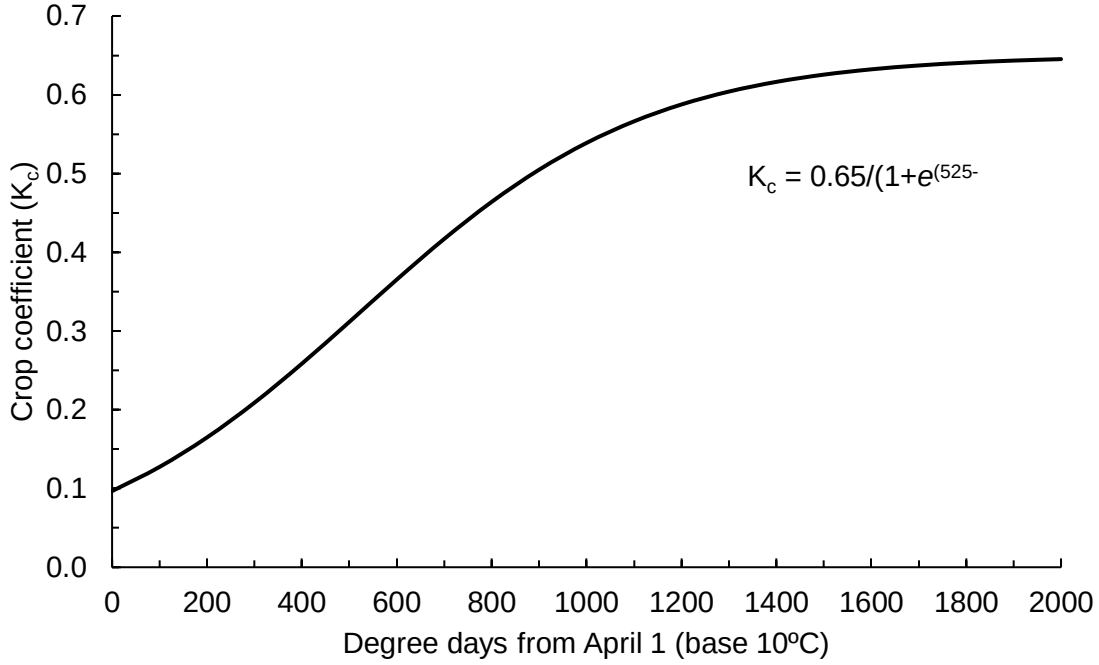

Figure 2. Daily degree days (DDs; base 10ºC) over the course of the growing season in 2017 and 2018. Black line is daily DDs and blue lines are weekly smoothed averages.

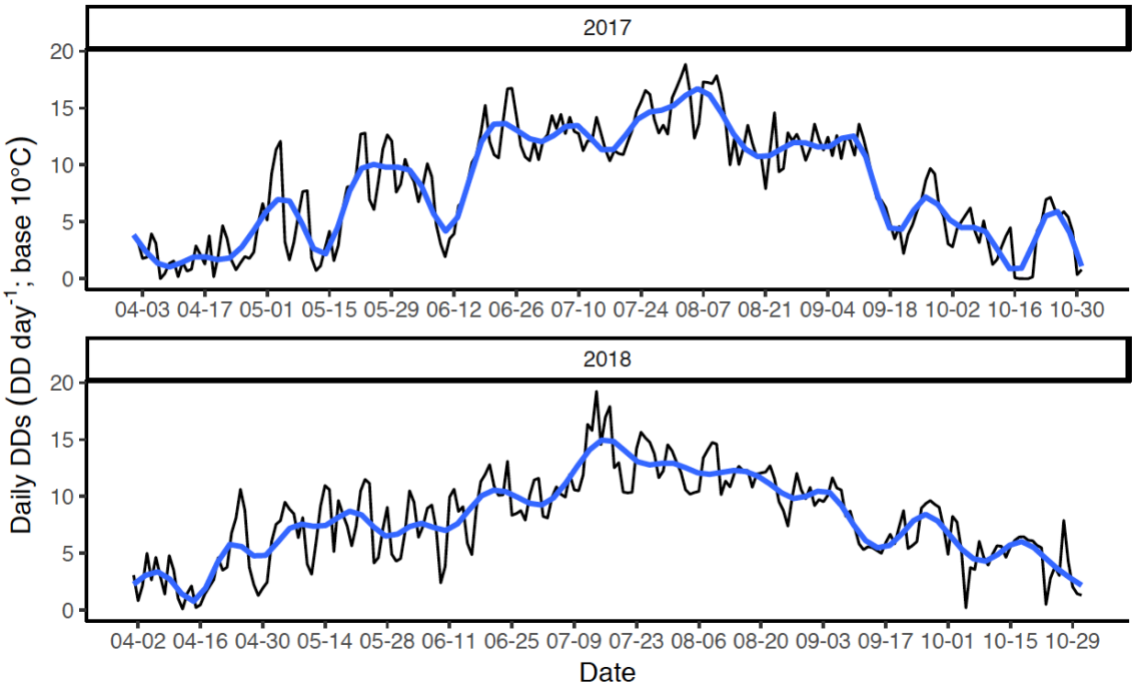

Figure 3. Daily precipitation (mm day^{-1}) over the course of the growing season in 2017 and 2018.

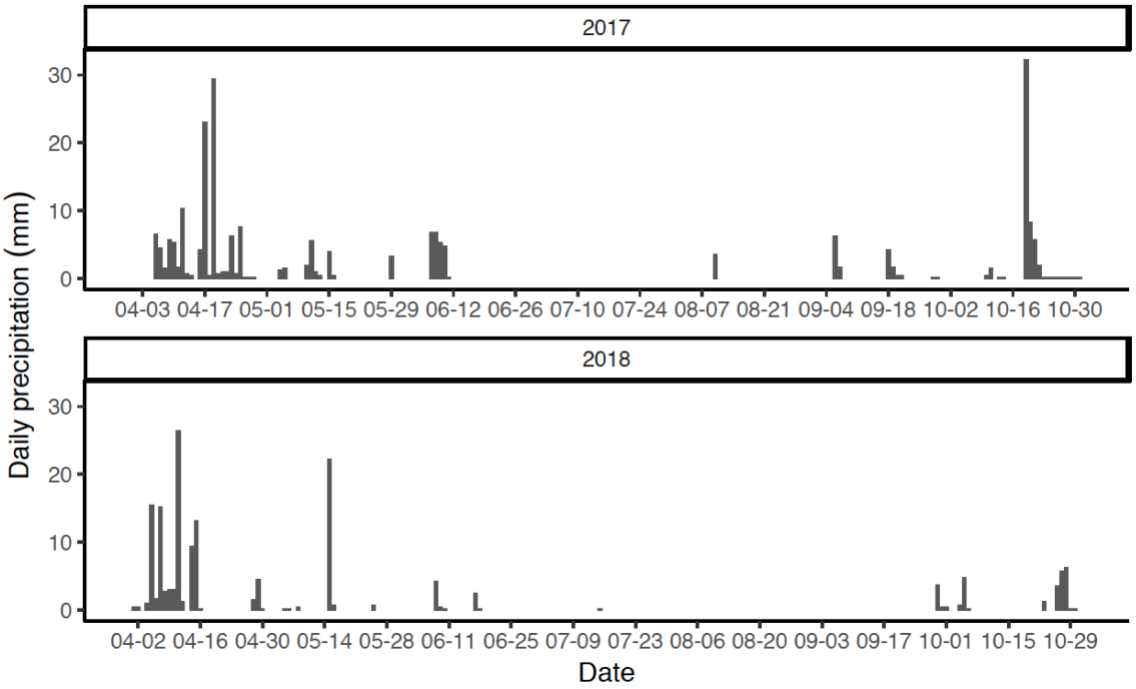

Figure 4. Daily reference evapotranspiration (ET_o; mm day^{-1}) over the course of the growing season in 2017 and 2018. Black line is daily ET_o and blue lines are weekly smoothed averages.

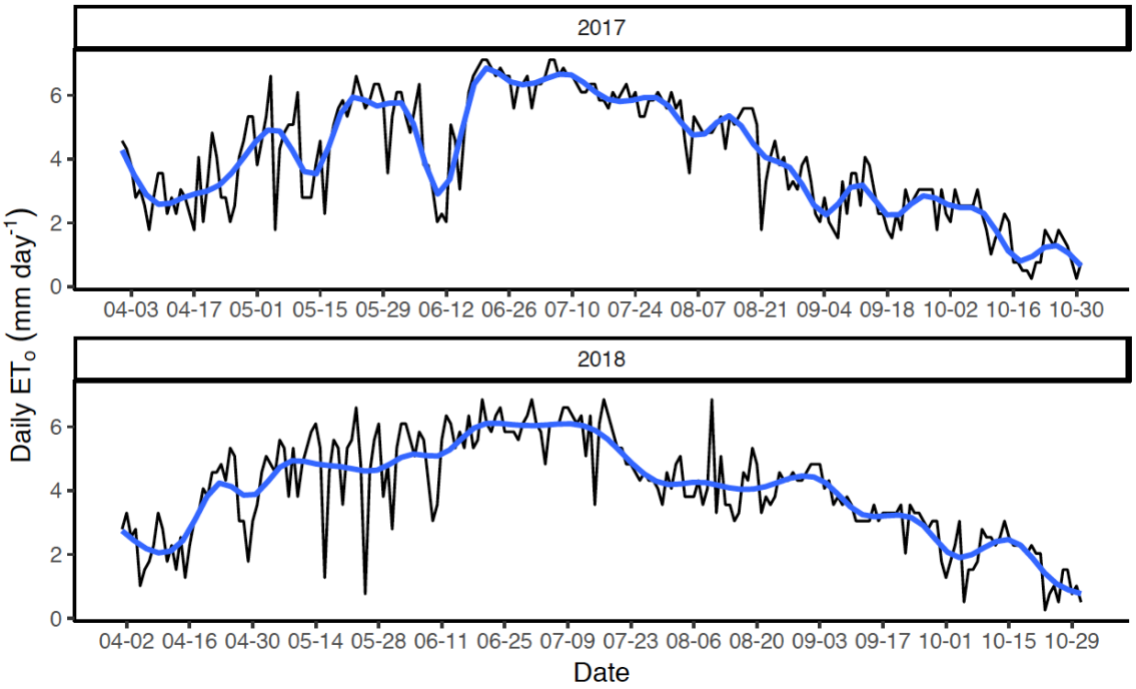

Figure 5. Daily estimated crop evapotranspiration (ET_c; mm day^{-1}) over the course of the growing season in 2017 and 2018. Black line is daily ET_c and blue lines are weekly smoothed averages.

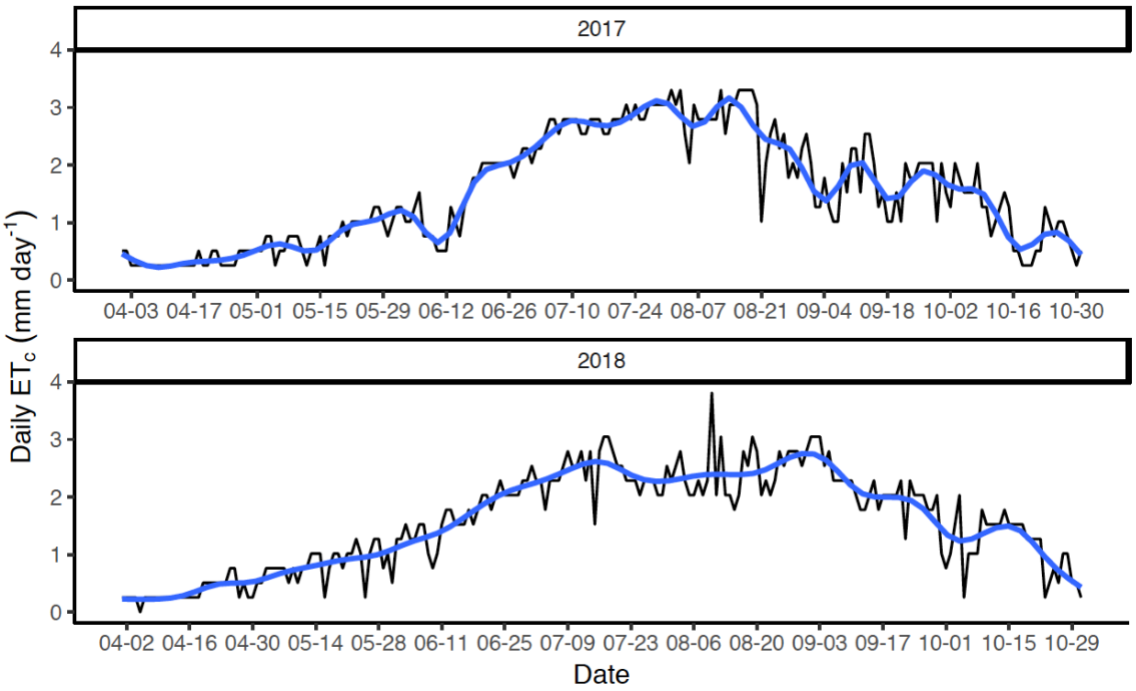

Figure 6. Seasonal time course of vine water status (Ψ_{stem}) in 2017 and 2018. Data points are means of the WC plots (n = 5) irrigated at 100% of estimated ET_c from onset of irrigation. Gray ribbons represent the 95% confidence limits of the means. Dotted lines represent the calculated non-stressed baseline Ψ_{stem} calculated from ambient temperature and relative humidity measured at the time of measurement.

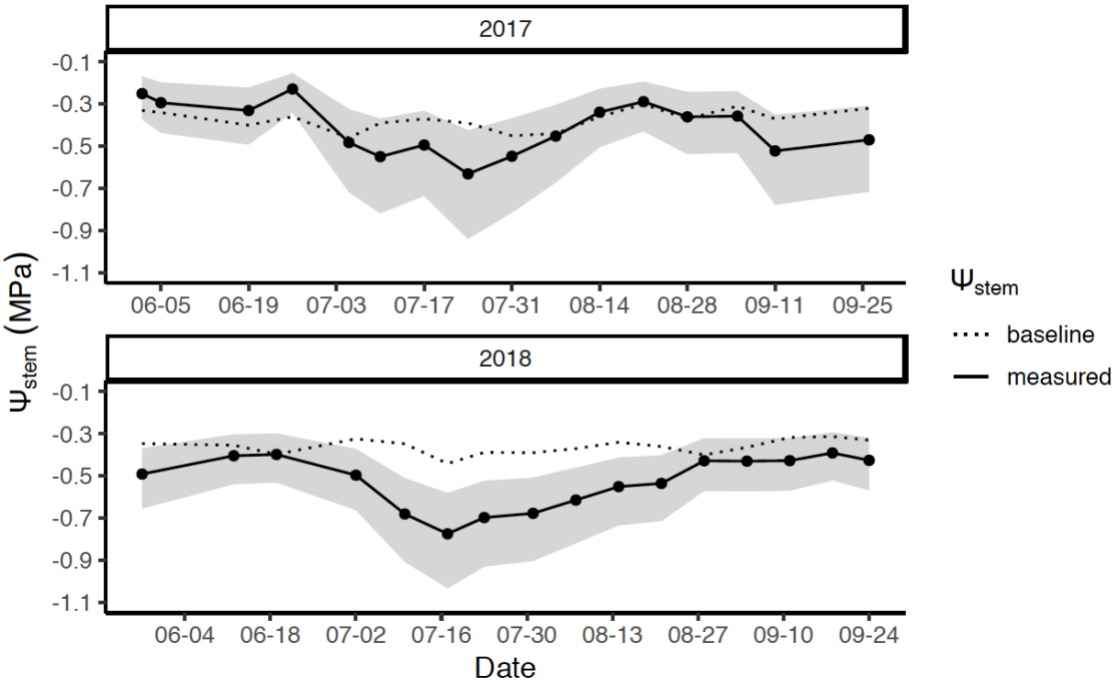

Figure 7. Mean shoot length as a function of days after budbreak over the course of the 2017 growing season. Data are means ± SEM (n = 5). Regression equation: $y = 162/(1+e^{((245-x)/73.8)})$; $R^2 = 0.99$.

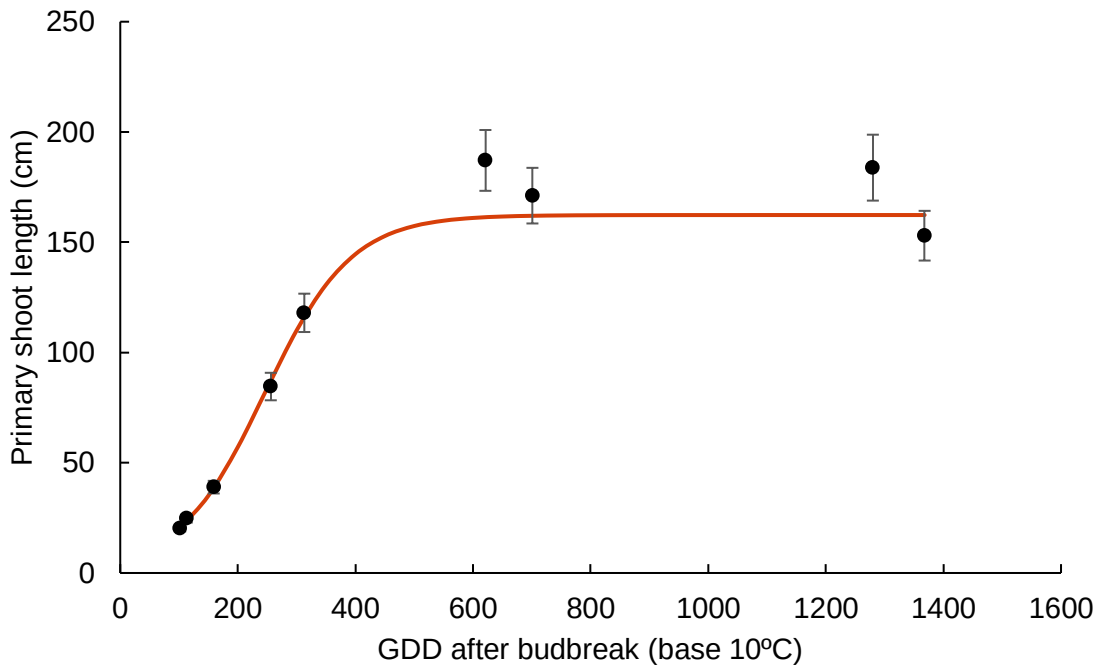

Figure 8. Mean primary, secondary, and total leaf area per vine over the course of the 2017 growing season. Data are means ± SEM (n = 5). Arrows indicate when vines were mechanically hedged (after measurements on 7/10/17 and 8/14/17, corresponding to 621 and 1280 GDD after budbreak, respectively). Those data points were excluded from the regression analyses.

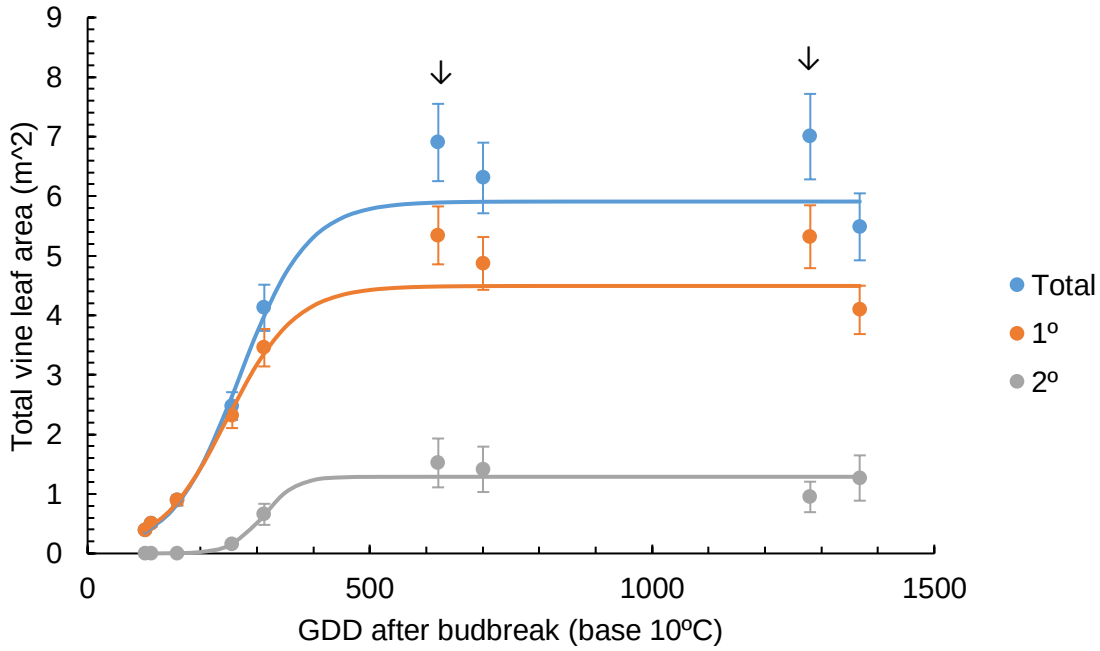

Figure 9. Total vine leaf area as a function of primary shoot length in 2017. Data are mean plot values ± SEM ($y = 0.040x - 0.606$; $R^2 = 0.997$, $P < 0.001$).

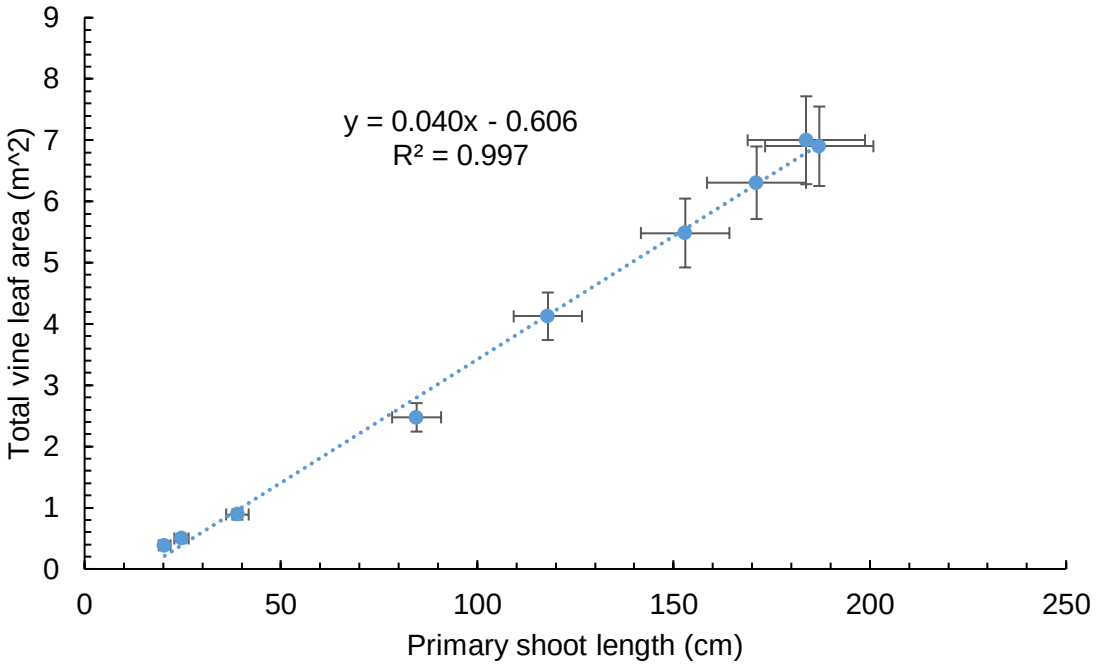

Figure 10. Seasonal evolution of canopy shaded area (%) as a function of GDD from budbreak for each measurement method over three seasons. Data area means ± SEM (n = 5).

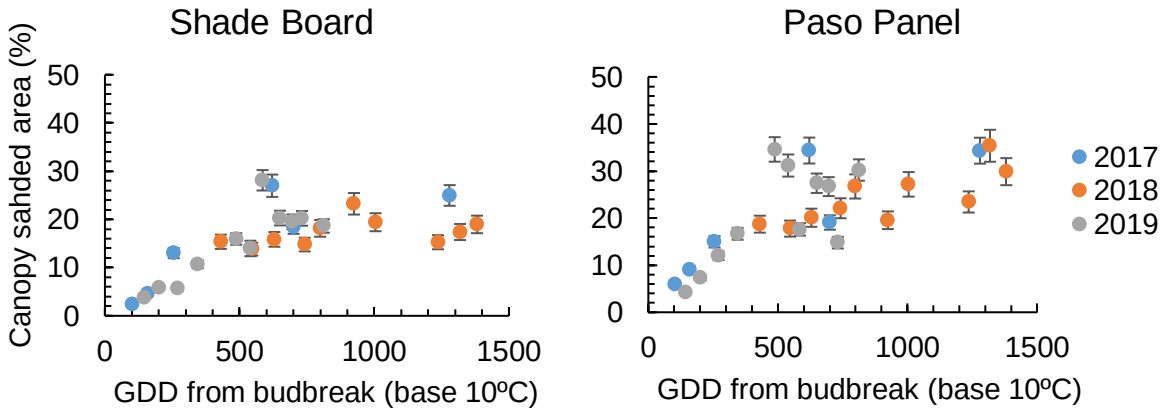

Figure 11. Canopy shaded area as a function of primary shoot length in 2017. Data are plot means ± SEM (n = 5).

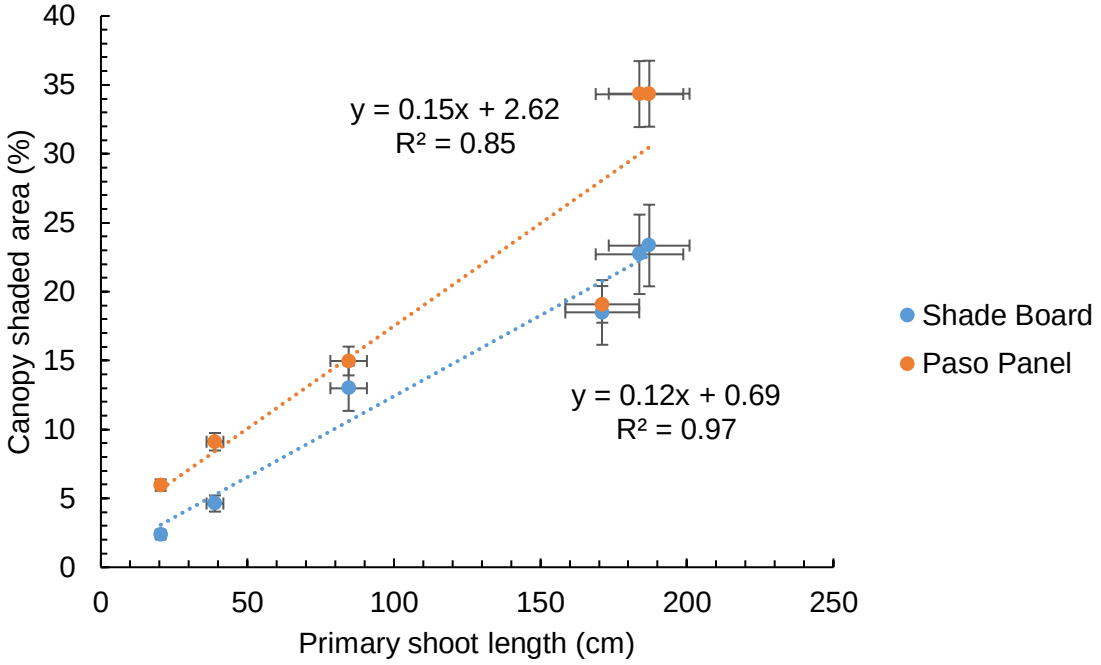

Figure 12. Canopy shaded area as a function of total leaf area per vine in 2017. Data are plot means ± SEM (n = 5).

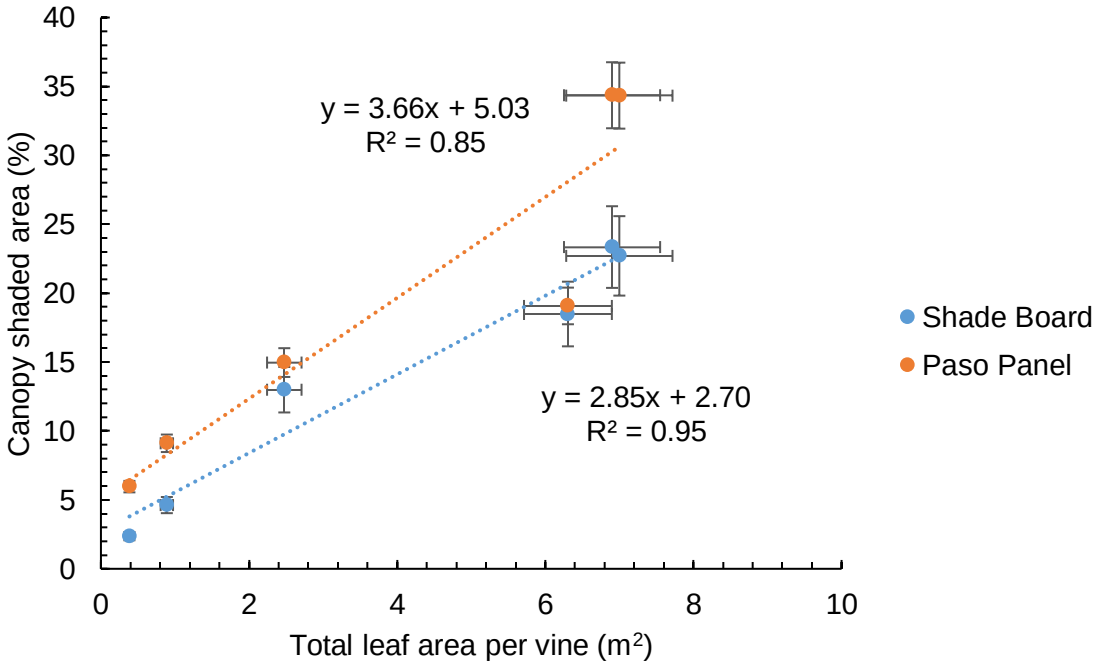

Figure 13. Canopy shaded area measured by Paso panel as a function of canopy shaded area as measured by shade board. Data are plot means (n = 5).

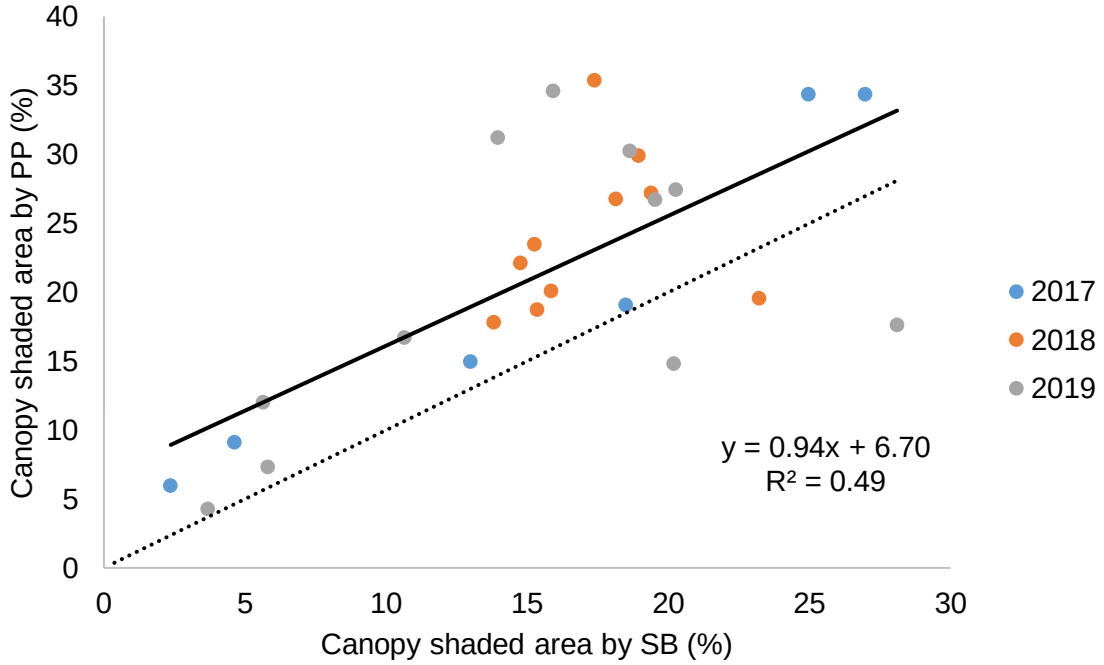

Figure 14. Crop coefficients as a function of degree-days after budbreak (GDD) developed from two methods of estimating vine canopy shaded area over three years of the study. Equations for functions are: PP – K_c = 0.46/(1 + e^((269.18 - GDD)/114.24)); and SB – K_c = 0.34/(1 + e^((294.35 - GDD)/104.90)).

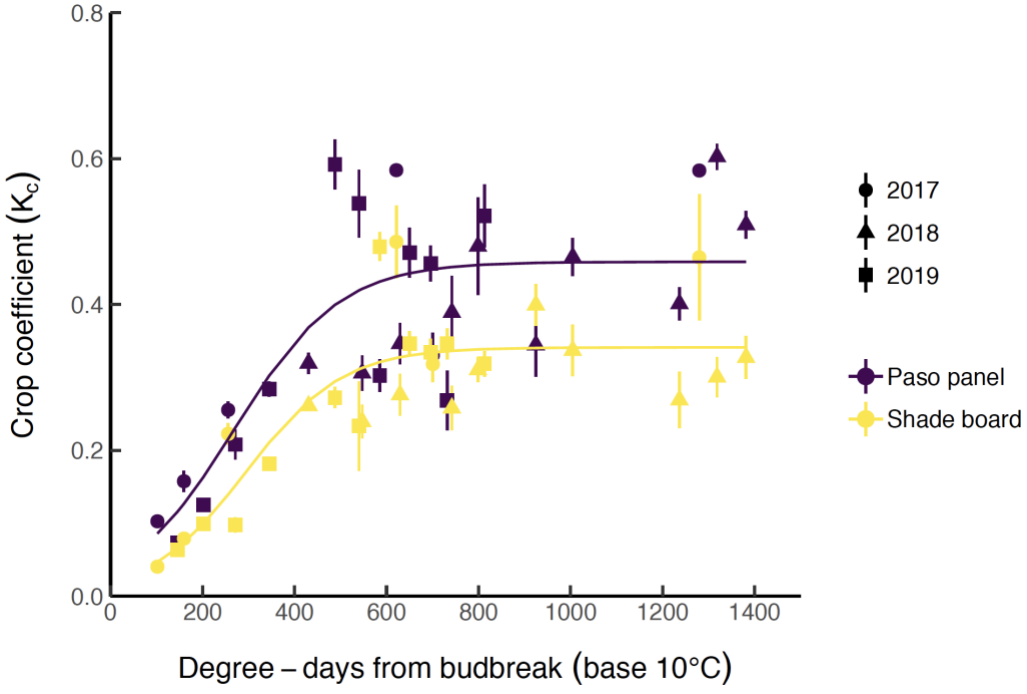

Figure 15. New crop coefficients (Kc) for each measurement method as a function of GDD from 1 April. PP – Paso panel; SB – Shade board.

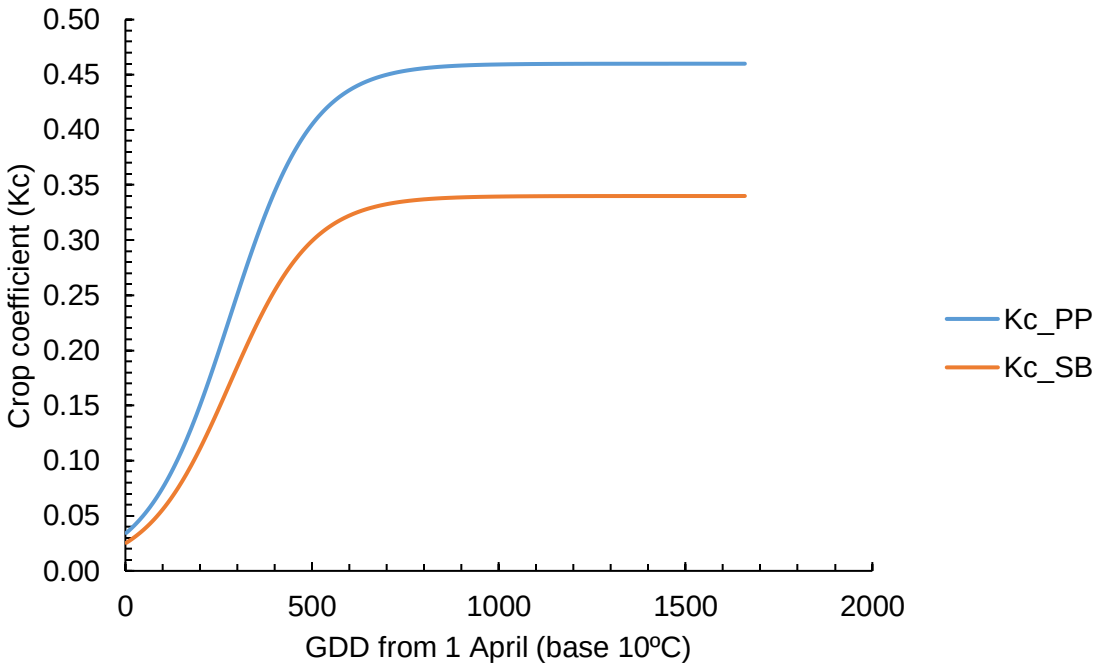

Figure 16. Modelled daily wine grape water use (ET_c) from 1 April to 31 October using 30-year averages for ET_o and GDD obtained from the AgriMet weather station located at SOREC. ET_o and GDD data are not shown, but used for the calculation of ET_c, whose equations were developed from this study (ETc_PP and ETc_SB) or taken from the literature (ETc_old).

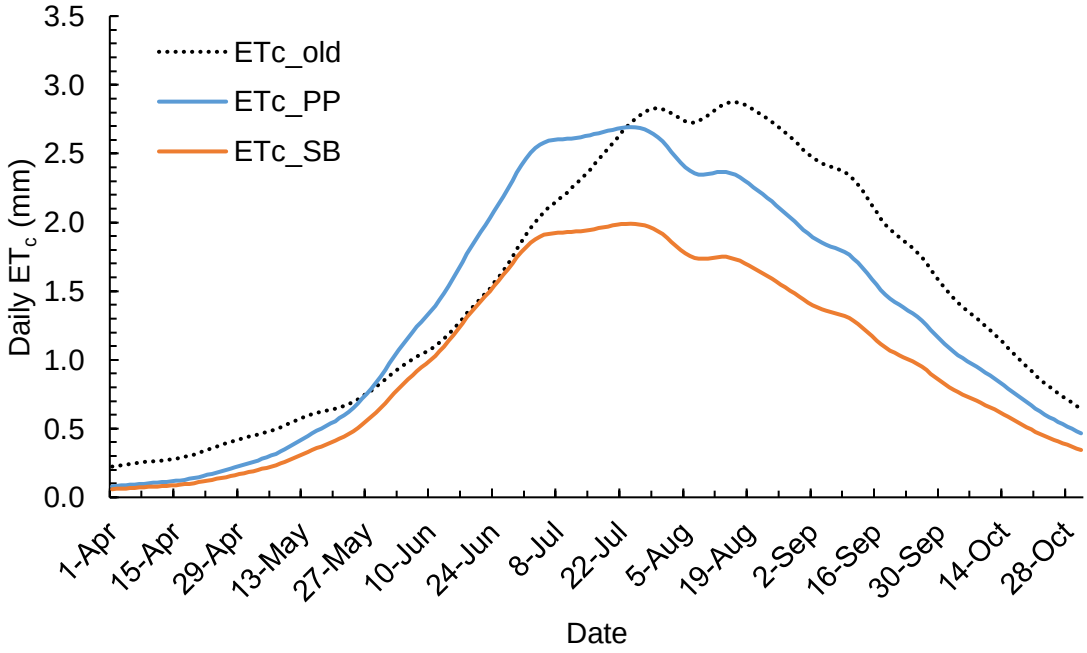

Table 1. Phenology of vines in 2017 and 2018.

Phenological event	2017		2018	
	Date	Days	Date	Days
Budbreak	17 April	--	23 April	--
Bloom	12 June	56	31 May	38
Veraison	14 August	63	13 August	74
Harvest	26 September	43	24 September	42
Bloom to Harvest		106		116
Budbreak to Harvest		162		154

Table 2. Applied water amounts during pre- and postveraison periods in each year of the study. Irrigation began on 10 July and 16 July in 2017 and 2018, respectively, once midday Ψ_{stem} reached -0.8 MPa when averaged across all plots in the experiment. Preveraison period began at treatment imposition and ended at veraison. Postveraison period began at veraison (14 and 13 August in 2017 and 2018, respectively) and ended at harvest in each year.

Year	Preveraison	Postveraison	Total
	---------- *liters vine*$^{-1}$ ----------		
2017	360	314	674
2018	318	443	761

Table 3. Results (*P* values) from Levene's ANOVA and regular ANOVA on the response of canopy percent shaded area to degree days, measurement method, and their interaction. Levene's ANOVA was conducted on the absolute values of model residuals.

	Levene's test			ANOVA		
Source	2017	2018	2019	2017	2018	2019
	---------- *P* value ----------					
Degree Days	0.060	0.147	0.059	<0.001	<0.001	<0.001
Method	0.930	0.274	0.702	<0.001	<0.001	<0.001
DD * M	0.077	0.144	0.124	<0.001	<0.001	<0.001

Table 4. Pairwise comparisons between measurement methods of canopy percent shaded area in each year of the study at each measurement date. *P*-values were adjusted using the Tukey-Kramer method. Estimates and standard errors (SE) are given on the log-scale. Positive estimate values indicate measured values were higher with the PP method, while negative estimate values indicate measured values were higher with SB method.

Year	GDD	Estimate	SE	df	*T* ratio	*P* value
2017	102	0.92	0.08	41.94	11.15	<0.001
	159	0.68	0.08	41.94	8.19	<0.001
	256	0.14	0.08	41.94	1.70	0.096
	621	0.24	0.09	42.04	2.74	0.009
	701	0.03	0.08	41.94	0.38	0.709
	1280	0.32	0.09	42.04	3.61	<0.001
2018	430	0.20	0.09	76.00	2.29	0.025
	547	0.25	0.09	76.00	2.90	0.005
	629	0.24	0.09	76.00	2.73	0.008
	742	0.40	0.09	76.00	4.64	<0.001
	799	0.39	0.09	76.00	4.47	<0.001
	925	-0.17	0.09	76.00	-1.99	0.051
	1005	0.34	0.09	76.00	3.88	<0.001
	1237	0.43	0.09	76.00	4.95	<0.001
	1318	0.71	0.09	76.00	8.20	<0.001
	1382	0.46	0.09	76.00	5.25	<0.001
2019	145	0.14	0.10	79.95	1.41	0.163
	201	0.23	0.10	79.95	2.32	0.023
	271	0.75	0.10	79.95	7.64	<0.001
	345	0.45	0.10	79.95	4.54	<0.001
	488	0.78	0.10	79.95	7.86	<0.001
	540	0.80	0.13	80.67	6.10	<0.001
	585	-0.47	0.10	79.95	-4.74	<0.001
	650	0.30	0.10	79.95	3.06	0.003
	696	0.31	0.10	79.95	3.16	0.002
	732	-0.31	0.10	80.15	-2.98	0.004
	813	0.48	0.10	79.95	4.90	<0.001

Table 6. Parameter estimates, standard errors (SE), and 95% confidence limits from non-linear sigmoidal fits for each measurement method. Treatment codes: PP = Paso Panel; SB = Shade Board.

Parameter	Method	Estimate	SE	Lower 95% CL	Upper 95% CL
K_c^{max}	PP	0.46	0.02	0.41	0.50
	SB	0.34	0.02	0.30	0.39
K_c^{50}	PP	269.18	19.43	230.93	307.44
	SB	294.35	25.01	245.10	343.60
Scalar	PP	114.24	18.33	78.14	150.34
	SB	104.90	22.01	61.56	148.24

Table 7. Pairwise comparisons between measurement methods of parameter estimates from non-linear sigmoidal fits. Show are contrast estimates, standard errors (SE), *T* ratio, and *P* values. Positive estimate values indicate measured values were higher with the PP method, while negative estimate values indicate measured values were higher with SB method.

Parameter	Estimate	SE	*T* ratio	*P* value
K_c^{max}	0.12	0.02	6.83	0.0001
K_c^{50}	-25.16	30.72	-0.82	0.4134
Scalar	9.34	28.59	0.33	0.7443

Table 8. Parameter estimates, standard errors (SE), and 95% confidence limits from new non-linear sigmoidal fits for each measurement method. Treatment codes: PP = Paso Panel; SB = Shade Board.

Parameter	Method	Estimate	SE	Lower 95% CL	Upper 95% CL
K_c^{max}	PP	0.46	0.02	0.42	0.50
	SB	0.34	0.02	0.30	0.38
K_c^{50}	overall	279.75	14.86	250.50	309.01

Scalar	overall	110.35	14.16	82.47	138.23